



Technical note

Non-contact position control via fluid shear force



Edward Sung^{a,*}, Brandon Chalifoux^a, Jay Fucetola^a, Mark L. Schattenburg^b,
Ralf K. Heilmann^b

^a Department of Mechanical Engineering, Massachusetts Institute of Technology, 70 Vassar St. 37-276, Cambridge, MA 02139, USA

^b Space Nanotechnology Lab, MIT Kavli Institute, 70 Vassar St. 37-276, Cambridge, MA 02139, USA

ARTICLE INFO

Article history:

Received 21 February 2014

Received in revised form 8 February 2016

Accepted 25 February 2016

Available online 11 March 2016

Keywords:

Non-contact

Shear force

Air bearing

Slumping

Glass

Machine vision

High temperature

ABSTRACT

Non-contact position control of components is beneficial to avoid wear, damage, and nonlinearities associated with friction. Air bearings, in particular, offer non-contact, high stiffness guidance, but no means of controlling the position of the supported component. In this work, we investigate the use of shear force resulting from the air bearing fluid flow as a means of actuation. Shear force actuation is tested in an air bearing slumping system, where a flat, horizontally placed glass substrate is supported on both sides by top and bottom air bearings. We investigate the use of two methods of substrate position sensing: a fiber-optic sensor and a machine vision sensor. We show that the glass substrate position can be successfully controlled by using fluid shear force. The magnitude of the fluid shear force is measured. System identification is performed, and the results are shown to agree with a second-order model.

© 2016 Elsevier Inc. All rights reserved.

1. Introduction

Frictionless mechanical elements and actuators are highly desirable in precision machines, where nonlinearity and hysteresis arising from friction can have a significant impact on positioning repeatability and accuracy. While frictionless guidance elements, such as flexures, magnetic bearings, and air bearings, can guide structures with excellent repeatability, the actuators themselves typically introduce friction and stress concentrations.

Air bearings are generally used with gaps smaller than 10 μm and provide nearly frictionless bearings [1]. Viscous forces are dominant over inertial forces in thin, long gaps in which the lubrication approximation is valid [2]. In lubrication flows, the fluid can support large loads and impart significant shear force on the object surface. When a planar air bearing is perfectly parallel to an object surface, the pressure distribution, and therefore the flow, of the fluid film is radially symmetric, so there is no net shear force on the surface. If a wedge angle is imparted, the shear forces become asymmetric due to a shifting pressure distribution [3], and a net shear force

arises. This concept is shown in Fig. 1, and has been modeled in Ref. [4]. Since this shear force is applied over the entire surface, stress concentrations are avoided. Devitt et al. [5] have reported using shear force as an actuation method for flexible films moving over cylindrical air bearings, to control tension of the film and to provide increased cooling, cleaning and drying of the film. van Rij et al. [6] and van Ostayen et al. [7] have used shear stress to control wafer position, by implanting an air bearing with many cells whose pressures may be independently controlled. This allows control of the direction of flow. The same effect may be achieved more simply, for our purposes, by wedging a top and bottom air bearing with the wafer in between, which is the method investigated in this work.

The motivation for the present work is to investigate the use of fluid shear force for actuation in a non-contact glass slumping device using air bearings, which is to be used in the fabrication of high-precision thin optics for X-ray telescopes. In this application, a flat, round glass substrate floats between two porous air bearings, and, as the device and glass are heated, the glass softens and conforms to the figure of the air bearings. The method of actuation researched by van Rij et al. [6] and van Ostayen et al. [7] cannot be used for slumping, because the softened glass at high temperatures will droop and touch the bearing, if it is not supported on both sides symmetrically.

Position control is required because the glass is in an unstable equilibrium. It is critical to have non-contact position actuation and sensing, which does not induce stress concentrations, in order to

* Corresponding author at: 1101 S Main St Apt 310, Milpitas, CA 95035, USA. Tel.: +1 650 630 8829

E-mail addresses: edsung89@gmail.com (E. Sung), bchal@mit.edu (B. Chalifoux), fucetola@mit.edu (J. Fucetola), marks@space.mit.edu (M.L. Schattenburg), ralf@space.mit.edu (R.K. Heilmann).

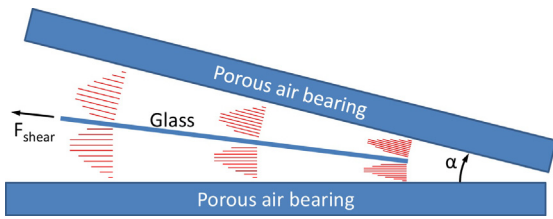


Fig. 1. Illustration of net shear force arising from wedge angle, α .

avoid introducing deformations in the glass, which can arise from even small concentrated forces while the glass is soft. For example, the simplest method to keep the glass centered in between the two bearings would be to add a physical stop around the circumference. However, it was discovered that any such physical stop, which is a small concentrated force, induces ripples in the glass geometry.

Non-contact slumping offers a distinct advantage over traditional contact slumping: mid-spatial frequency errors are not introduced. In contact slumping, glass is placed on a mandrel, with a release layer between the two (to prevent the glass from fusing to the mandrel), and heated to the softening point of the glass. Gravity forces the glass to conform to the figure of the mandrel, but any non-uniformity of the release layer, due to either clumping or dust particles, introduces mid-spatial frequency errors in the slumped glass. These errors adversely affect the angular resolution of X-ray telescopes, and are difficult or impossible to remove using figure correction techniques [8]. Non-contact slumping on air bearings avoids this issue by replacing the solid or powder release layer with an air film. In addition to not introducing ripples, this air film allows significantly faster slumping cycles since the glass is not in contact with a mandrel, which is a large mass with a significantly different coefficient of thermal expansion than that of glass. A long cool-down time, on the order of days, is required to minimize figure errors due to this mismatch in the coefficients of thermal expansion.

2. Slumping device prototype design

Investigating the use of shear force as a means of position control requires a device with air bearings capable of supporting a glass substrate and imparting a controllable wedge angle to generate shear forces. The device shown in Figs. 2–4 is a non-slumping (room temperature) prototype that is meant to only validate the usage of fluid shear force as an actuator. This initial device does not need to actually slump glass, so it does not need to withstand high temperatures. Although the method of position sensing used in the

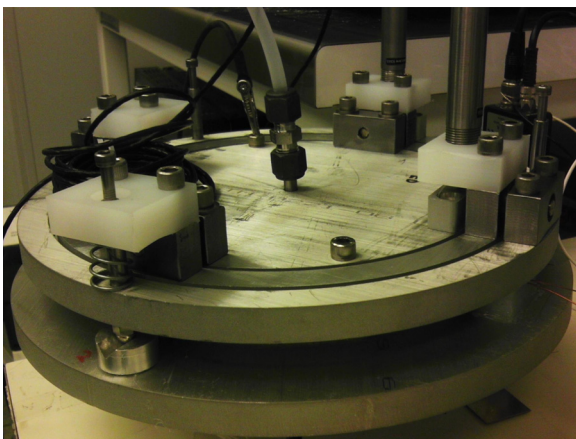


Fig. 2. Photo of device used to control glass position between two air bearings.

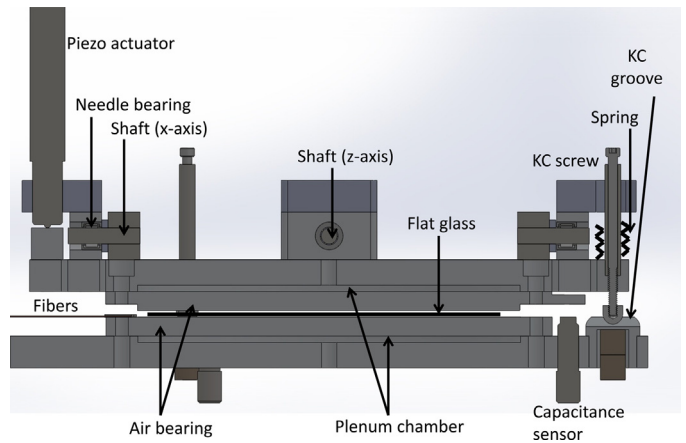


Fig. 3. Cross-sectional view of the device in a perfectly stable position.

600 °C application is presented in Section 2.2, the complete design of the final slumping (high temperature) device is not presented in this paper.

2.1. Mechanical design

The slumping device, described in detail by [9], can be divided into two subassemblies, top and bottom, which are mated together through an adjustable kinematic coupling (KC). The purpose of the kinematic coupling is to enable repeatable positioning of the subassemblies with respect to each other after removal of the top assembly for maintenance. Each subassembly holds a porous air bearing and a plenum chamber. The two air bearings face each other with a tightly controlled gap, in which a substrate is placed. The bottom subassembly stays stationary and provides the bottom support for the substrate. The top subassembly works as a 2-axis gimbal to angle the top air bearing in relation to the bottom bearing to provide a directed shear force.

Fig. 5 illustrates the exaggerated kinematics of the top subassembly. The outer ring mates to the bottom subassembly using the KC adjuster screws, which rest in the KC grooves on the bottom subassembly. The outer ring remains stationary, while the inner ring and bearing/plenum combination each provides rotation about a quasi-horizontal axis (x and z axes). Three capacitance sensors (HPT-150F-V-N2-3-B “V” series probes from Capacitac) are mounted to the bottom subassembly, and provide

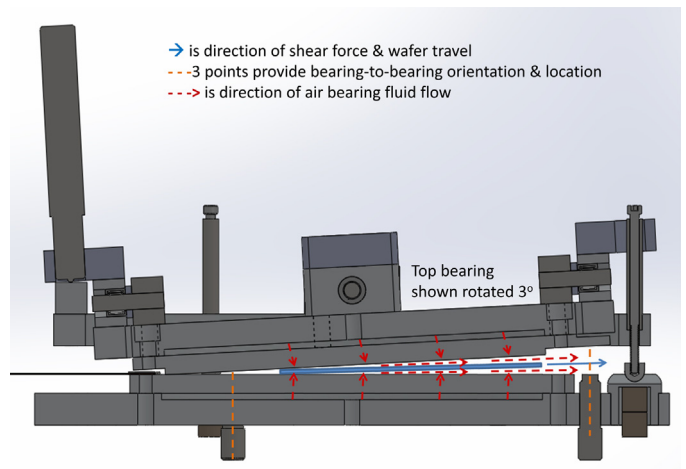


Fig. 4. Cross-sectional view of the device illustrating rotation of the top bearing to impart a shear force.

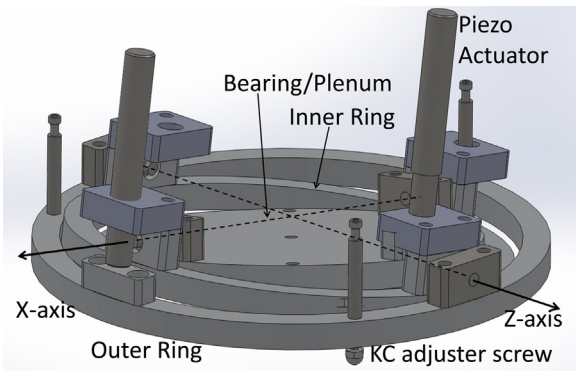


Fig. 5. Top subassembly of device with exaggerated movements.

bearing-to-bearing gap distances at 3 points to calculate the overall bearing-to-bearing angle. These capacitance sensors were calibrated to have a resolution of 87.5 nm with a measurement range of 2.5 mm. Two stack-type piezoelectric actuators (P/N PA100/T14 from Piezosystem Jena), which are mounted on the inner ring, push on the outer ring and the bearing/plenum separately to provide the rotational movements. They feature a range of motion of 105 μm, and a resolution of 0.21 nm.

Machined porous aluminum is used as the air bearing material, and the bearings are lightly held to the plenums with screws and sealed around the edges using adhesives. The plenum pressure is limited to about 1 psi to minimize bowing of the bearing.

2.2. Fiber-optic sensor

A fiber optic sensor, described in detail in Ref. [9] and shown in Fig. 6, was developed to provide substrate position feedback in anticipation of using this sensor at temperatures suitable for slumping (i.e. 600 °C). 15 mW of 850 nm wavelength light is fed into a fiber with a 500 μm core diameter, and is directed normal to the edge (cylindrical surface) of the substrate. The reflected light is picked up by another fiber located next to the source fiber, and is detected by a silicon photodetector. The reflected light intensity is found to be an exponential function of distance, as shown in Fig. 6. The range of the usable signal is 3–10 mm from the ends of the fibers.

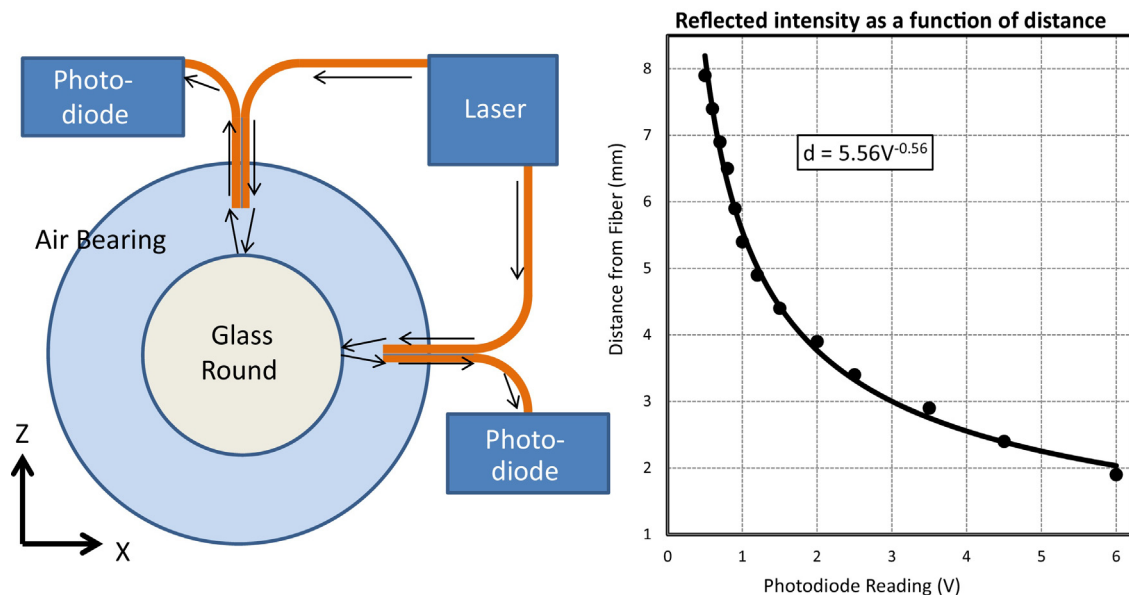


Fig. 6. Fiber sensor concept for glass position measurement, and measured reflected intensity as a function of distance from fiber. Measurements taken under static conditions.

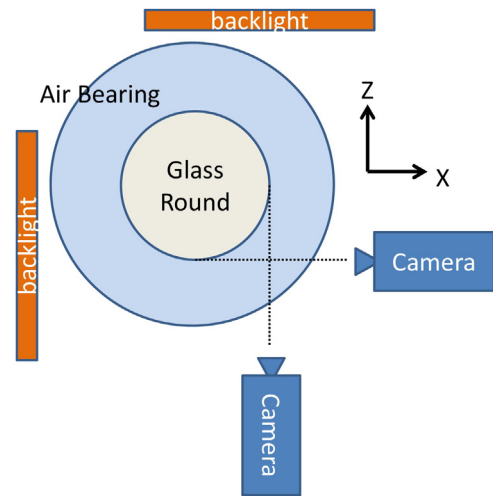


Fig. 7. Schematic of machine vision glass position measurement system.

The main limitation of this sensor is its sensitivity to edge defects. Glass wafers are typically only polished on the flat surfaces and have highly irregular edge surfaces. Thus, as the wafer translates or spins, the light that reflects off the edge and into the detection fiber fluctuates heavily, introducing significant noise. With heavy low-pass filtering, this sensor was found to be sufficient for coarse position control at high temperature [9], but insufficient for characterization of the shear force. For the purposes of characterization of the shear force, a machine vision system was implemented, as described in Section 2.3. However, in a high temperature slumping device, which operates at 600 °C, the fiber optic sensor is used instead of the machine vision system.

2.3. Machine vision

Machine vision was implemented as a better method of position measurement at room temperature. The glass substrate is backlit with a cold cathode tube diffuse light source along two axes, and the position measured with a CCD camera in each axis, as shown in Fig. 7. The image is dark where the glass blocks the light, and it is bright elsewhere. To determine the edge position of the glass, we

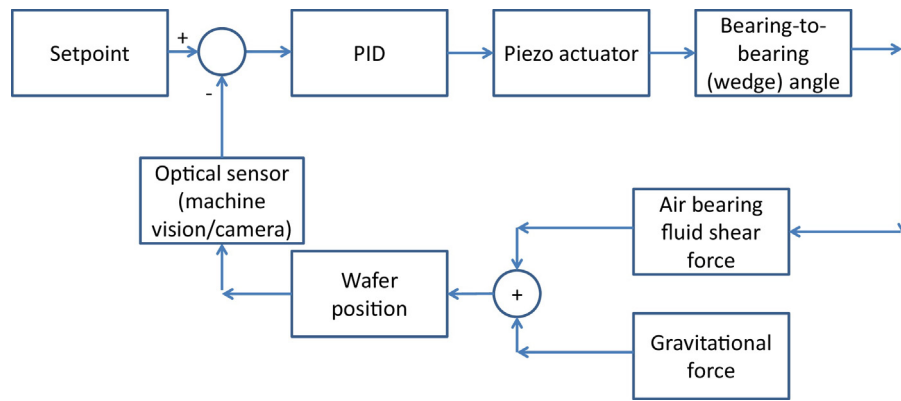


Fig. 8. Block diagram of system with PID control loop.

find the peak of the cross-correlation between the image and a step function. This reliably located the edge to the nearest whole pixel.

The range of this position measurement is approximately 25 mm in each axis, and the glass position resolution is around $75 \mu\text{m}$ (1 pixel). With this system, the edge quality of the glass introduces no significant noise; the noise is less than 1 pixel. Reliable position measurements of sufficient accuracy for our application were achieved with this system, so it was used for the shear force characterization and transfer function measurement described in this paper.

3. Experimental

The experimental objectives were to: (1) understand the nature of the shear force and measure its magnitude; and (2) to understand the system dynamics and measure the frequency response. The shear force is found to vary linearly with wedge angle. Measuring the magnitude of this force is important for understanding how well the glass position can be controlled by this force. In all of these experiments, the position of the glass was controlled with a PID controller, using the machine vision system for positional feedback. Based on the feedback of the machine vision, a PID-controlled voltage was outputted to the piezo-electric actuators, which changed the wedge angle, thus creating a directed fluid shear force on the glass. The PID controller used for glass position control was not optimized, but provided glass position stability to allow a frequency response measurement. Section 3.3 discusses the frequency response measurement of the system. The controller operates at a sampling frequency of 40 Hz, and the response is at most 1 Hz. Fig. 8 shows a block diagram of the system, including the PID input.

3.1. Shear force measurement

The purpose of this experiment was to measure the shear force, T , as a function of wedge angle, α . The average gap between each bearing and the glass was held constant at $30 \mu\text{m}$ (minimum distance from center of bearing to glass). While smaller gaps would provide higher fluid shear force, we chose a larger gap in order to perform the experiments over a larger wedge angle.

The position of the glass was held constant near the center of the bearings using PID control, and the entire assembly was tilted over a range of $\pm 800 \mu\text{rad}$ from horizontal as measured by a precision bubble level. As the tilt angle increases, the wedge angle also increases, in order to create a greater fluid shear force. The steady state wedge angle between bearings was measured using the capacitance sensors. At the steady state wedge angle, α , for a given tilt angle θ , the glass is in static equilibrium, and the shear

force at this wedge angle is equal to the component of the gravitational force parallel to the glass sheet:

$$T = m_{\text{glass}} * g * \sin(\theta) \quad (1)$$

The measurements from the experiment gave us the relationship between α and θ , and substituting into Eq. (1), we can further formulate the relationship between T and α . As shown in Fig. 9, the shear force is a linear function of wedge angle, and is measured as:

$$T = [0.54 \mu\text{N}/\mu\text{rad}]\alpha \quad (2)$$

Data from [5] suggest a shear force constant around $50 \mu\text{N}/\mu\text{rad}$, for a flat graphite bearing at 60 psi plenum pressure. However, the experimental setup of [5] is very different from the present study in that, in [5], the “bottom bearing” is actually an air bearing roller, and the “substrate” is a thin sheet of plastic constrained by 3 rollers. The flat graphite bearing was pressed against a round surface, which does not provide a large flat surface – only a relatively small surface area would be effective in providing a shear force. In addition, our plenum pressure is much lower (1 psi), so a direct comparison of our results is invalid. Thus we mention this information only as a rough verification that our measurements appear to be in a similar regime.

3.2. Spring constant measurement

When the slumping device is well-leveled and the wedge angle is zero, the glass substrate finds an equilibrium position, contrary to our previous statement that the system has an unsteady

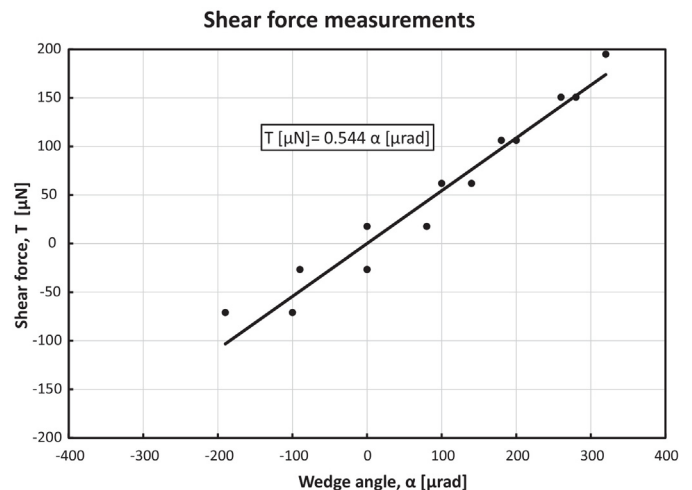


Fig. 9. Measured shear force as a function of wedge angle, α .

equilibrium. As the bearings are held constant with respect to each other, and the entire assembly is tilted, the position of static equilibrium changes, and the change in position is proportional to the force applied to it (in this case, misalignment with gravity): a spring force. The spring force is relatively small, however, and cannot be relied upon to keep the glass in position under changing conditions (i.e. thermal expansions during ramp-up to 600 °C). Even a tilt of just 0.5° will cause the wafer to fall/slide out from between the bearings. This behavior is also observed when the tilt angle is kept constant but the wedge angle is varied (as we saw in Section 3.1, this also changes the force applied to the glass). This phenomenon is not yet fully understood.

The purpose of this experiment was to measure the spring constant of the system. While in the previous experiment, the glass position was the variable that was held constant, in this experiment, it is the wedge angle that was held constant. That is because the effect of shear force via a wedge angle needed to be eliminated.

The glass position controller was turned off, and the wedge angle controller was commanded to maintain a constant wedge angle. The machine vision camera was left on to record the position of the glass. The entire assembly was tilted, and the inclination angle was measured with precision levels. At each inclination angle, the glass moves to a new equilibrium position, where the spring force and gravitational forces are equal. The relationship for spring force can be substituted into Eq. (1) in order to relate the spring force to the tilt angle:

$$F_{\text{spring}} = k * x = m_{\text{glass}} * g * \sin(\theta) \tag{3}$$

The data in Fig. 10 shows that position is a linear function of tilt angle. The spring constant is found to be very small: 18.46 μN/mm.

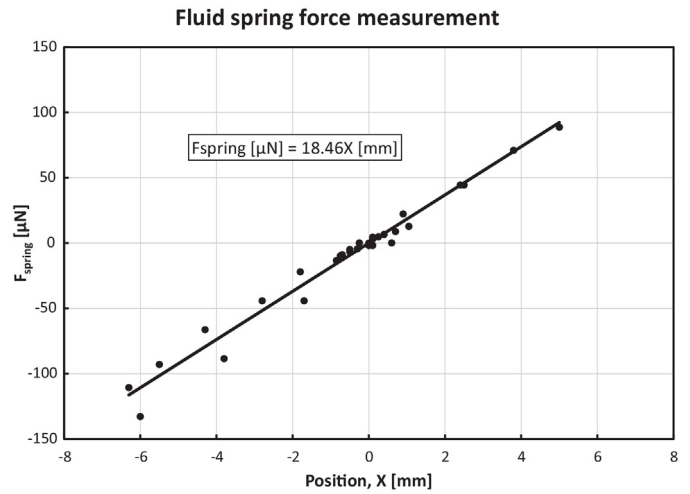


Fig. 10. Measured fluid spring force as a function of glass position.

3.3. Frequency response measurement

In order to understand this system, it is useful to measure the frequency response. The system was excited with a sinusoidal force and sinusoidal response was measured. Since it was found that shear force is linearly related to wedge angle, we applied a sinusoidal wedge angle on one axis. The amplitude was 50 μrad and the frequency varied between 0.01 Hz and 1 Hz. The position of the glass was measured using the machine vision system, operating at a sampling frequency of 40 Hz, with a time delay of 2.4 ms between the wedge angle measurement and the image acquisition.

During system identification, the position of the glass was uncontrolled in the measured axis, and controlled using a PID

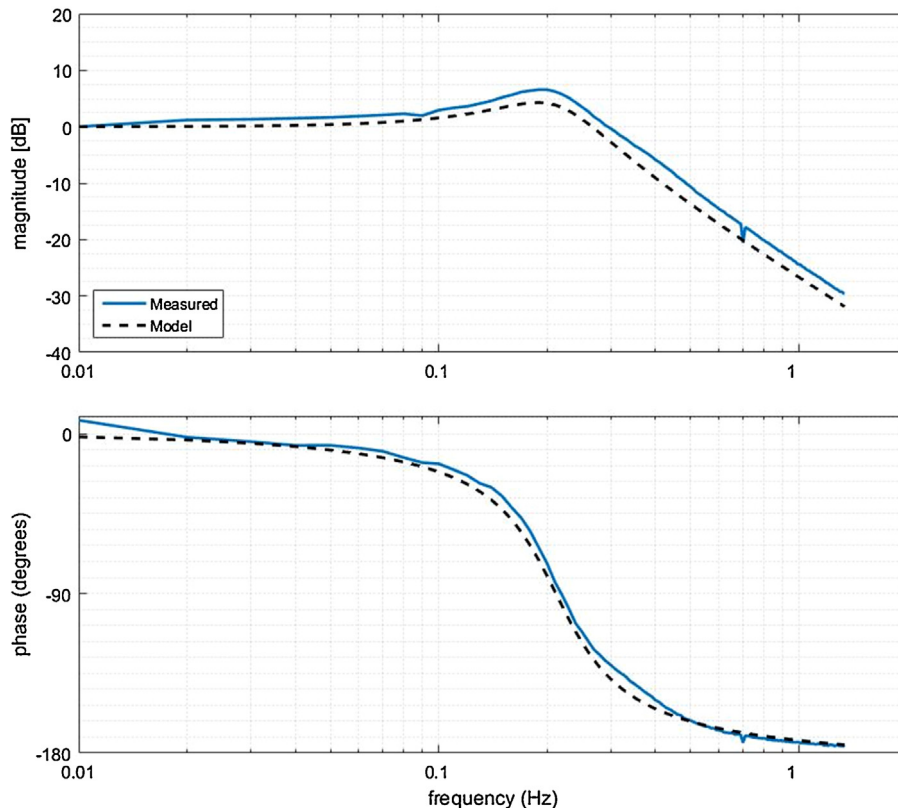


Fig. 11. Magnitude (top) and phase (bottom) plots of measured and model plant transfer functions, using machine vision position measurement system.

controller in the orthogonal axis. The magnitude and phase of the response is measured using 10–100 excitation cycles at each frequency, and the frequency response generated as shown in Fig. 11. The model shown is discussed in Section 3.4.

3.4. Dynamic system model

This system can be represented by a mass-spring-damper system with a time delay, with a two-pole transfer function:

$$G(s) = \frac{x_{\text{glass}}(s)}{\alpha(s)} = \frac{G(0)\omega_n^2}{s^2 + 2\omega_n\xi s + \omega_n^2} e^{-\tau_{\text{delay}}s} \quad (4)$$

where s is the frequency variable (in this case, $s = j\omega$), ω_n is the natural frequency, ξ is the damping ratio, τ_{delay} is a time delay between measurements of input (wedge angle) and output (glass position), and $G(0)$ is the static response. These parameters can be related to the mass, viscous friction, and spring constant of the system:

$$\omega_n = \sqrt{\frac{k}{m}}, \quad \xi = \frac{b}{2\sqrt{km}}, \quad G(0) = \frac{x}{\alpha} = \frac{T/k}{\alpha} \quad (5)$$

where k is the spring constant, m is the mass, b is the viscous friction parameter, and T is the static shear force on the glass due to bearing wedging, and was found in Section 3.1.

The viscous friction arises from Couette flow [2] between the bearings and the glass, due to the movement of the glass relative to the stationary bearings. Since the system is linear, the net shear force on the glass is a superposition of the force arising from the position-dependent force (spring force), the wedge-angle-dependent force (excitation force), and the velocity-dependent force (Couette flow). The viscous friction parameter, b , is computed from:

$$b = \frac{2A\mu}{h} \quad (6)$$

where A is the surface area of the glass, μ is the dynamic viscosity of the air, and h is the gap between the glass and bearings. The viscous friction parameter for nitrogen at room temperature ($\mu = 1.76 \times 10^{-5}$ Pa s), a gap of 30 μm , and a 100 mm diameter substrate is found to be 9.2×10^{-3} N s/m, according to Eq. (6). The glass substrate mass is measured to be 10.8 g. The spring force constant arises from the phenomena discussed in Section 3.2, and is measured to be 18.46 $\mu\text{N/mm}$. The shear force constant is measured in Section 3.1 to be 0.54 $\mu\text{N}/\mu\text{rad}$. From these four physical parameters, $\omega_n = 1.33$ rad/s, $\xi = 0.32$, and $G(0) = 0.0294$ mm/ μrad . This modeled transfer function is plotted along with the measured transfer function in Fig. 11.

4. Discussion

This system can adequately be described by mass-spring-damper system. The mass and viscous friction components are clear, but the cause of the spring phenomenon is not known. It may arise because the glass position affects the flow field in the bearing, since the glass does not completely cover the bearing. As the glass moves to one side, the flow on the other side of the bearing may increase, dragging more fluid toward that side, and providing a restoring force. This spring-like behavior was observed only when both bearings were present. If the glass is floating on the bottom bearing only, then the glass position is unstable. It is also clear that the spring force does not arise from a varying wedge angle, because in the experiment described in Section 3.2, the wedge angle was held constant, but the restoring force was observed.

The tolerance in the measurement of magnitude and phase during each experimental run is quite low, since at least 10 cycles were used for all frequencies. As the frequency increased and the response magnitude decreased, more cycles were used in calculating the response magnitude and phase. For example, at frequencies near 1 Hz, the amplitude of the response was only around 2 pixels, which would not have given an accurate measurement normally. To overcome this resolution limitation, the wafer pixel position was averaged over numerous cycles to gain a statistical measurement of position.

There is uncertainty in the plenum pressure used, due to leakages through the bearing and plenum mating surfaces. This makes the variation of shear force due to plenum pressure difficult to characterize. The tolerance in the gap between the bearings and glass is ± 5 μm due to capacitance sensor accuracy and wafer thickness measurement accuracy. This also limits our ability to study the variation of shear force with bearing gap.

5. Conclusions

In this work, we have demonstrated the use of shear force as a method of actuation to control the position of a flat glass substrate between two flat air bearings. The magnitude of the shear force has been quantified, and found to be linearly related to the wedge angle. In addition, the frequency response of the system has been measured, and shown to agree with a two-pole system model consisting of a mass, spring, and damper.

While the frequency response indicates that fast position control is not possible with the current design (e.g. low pressure), this is sufficient for control of a glass substrate during slumping, where the goal is to keep the glass stationary to within about 1 mm. At room temperature, our control system maintains position to less than ± 0.1 mm. In practice, the ability of the controller to maintain the glass position has been limited by the sensor noise. For other applications, there are other ways that shear force might be implemented. For example, air bearings supporting a stage or object could be tilted to provide a shear force, or a set of air bearings dedicated to providing shear force can be used.

Acknowledgement

The authors thank NASA grant NNX10AF59G for supporting and funding this research.

References

- [1] Slocum AH. Precision machine design. 1st ed. Michigan: Society of Manufacturing Engineers; 1992. p. 421–625.
- [2] Panton RL. Incompressible flow. 3rd ed. New Jersey: Wiley; 2005.
- [3] Rao NS. Analysis of aerostatic porous rectangular thrust bearings with offset loads. Wear 1980;59:333–44.
- [4] Hussein A [MS Thesis] Design and Modeling of a Third Generation Slumping Tool for X-ray Telescope Mirrors. Massachusetts Institute of Technology; 2011, June.
- [5] Devitt D, Allen J. Viscous shear in air bearings gaps for precise web tension and temperature control. Proc ASPE 2012.
- [6] van Rij J, Wesselingh J, van Ostayen R, van Eijk J. Planar wafer transport and positioning on an air film using a viscous traction principle. Tribol Int 2009;42:1542–9.
- [7] van Ostayen R, van Eijk J, Schmidt RHM. Contact-less thin substrate transport using viscous traction. Design, control, and software implementation for distributed MEMS (dMEMS). In: 2012 Second Workshop. 2012. p. 14–21.
- [8] Zhang W, Chan KW, McClelland RS, O'Dell SL, Saha TT. Next generation X-ray optics: high-resolution, light-weight, and low-cost. Proc SPIE 2012; 8443.
- [9] Sung E [MS Thesis] Horizontal Non-contact Slumping of Glass. Massachusetts Institute of Technology; 2013, May.